A Topology Based Approach for the Generation and Regularization of Roof Outlines in Airborne Laser Scanner Data

SANKA NIRODHA PERERA[1], HANS-GERD MAAS[1]

Abstract: In this paper, we present a new approach for the generation and regularization of 3D roof boundaries in Airborne Laser scanner (ALS) data. Initially, segment based classification approach is chosen to discriminate off-terrain points from the terrain points and different rules are then imposed to extract as much of roof planes. We introduce the use of cycle graphs to the roof topology graph. The Dijkstra's algorithm is used to recognize the possible shortest closed cycles, and used such cycles for the fixing of ridge-line intersections. The subdivision of cycles is performed to handle step-edge intersections whilst union of connected cycles are taken for the manipulation of outer roof boundaries. Experimented results show that our approach is promising and can be obtained topologically valid, complete 3D roof structures.

1   Introduction

1.1   General Remarks

Automated 3D building modeling is important for many applications such as city modeling and virtual reality, telecommunication, map updating and so on (SOHN & DOWMAN, 2007). Data, captured by Photogrammetric or LiDAR techniques, is basically used for the modeling schemes but, the latter source is promising as the point clouds have more automated potential though they are irregularly distributed. To date, there exist many strategies (e.g. MAAS & VOSSELMAN, 1999; BRENNER & HAALA, 1998; SCHWALBE ET AL., 2005; OUDE ELBERINK, 2010) for the reconstruction of the building models. However, the state of art of techniques in 3D building reconstruction is still being developed. Specially, in terms of the feature extraction based on the topology and the way of incorporating such features on building shapes in order to reconstruct a geometrically valid detailed polyhedral models. In this end, this paper presents a novel approach to make use of topological property of building roof segments and then to reconstruct 3D building roof structures based on the cycle graphs.

Authors, in this paper, take part of the ISPRS Test Project on Urban Classification and 3D Building Reconstruction in 2012 (ISPRS COMMISSION III, 2011) and thus data were obtained from the ISPRS commission III/4. It should be mentioned that the data were captured by the Leica ALS50 over the Vaihingen city, Germany.

1) Sanka Nirodha Perera, Institute of Photogrammetry and Remote Sensing, Technische Universität Dresden, Helmholtz Straße 10, 01069 Dresden, Germany; E-mail: sanka.perera@mailbox.tu-dresden.de
2) Hans-Gerd Maas, Institute of Photogrammetry and Remote Sensing, Technische Universität Dresden, Helmholtz Straße 10, 01069 Dresden, Germany; E-mail: hans-gerd.maas@tu-dresden.de

1.2   Related Work

Building reconstruction based on the intersection of neighboring planes, proposed by (MAAS & VOSSELMAN, 1999), provides the firm basement for many modeling schemes as both data driven and model driven approaches can be linked with the information of intersection edges or ridgelines. Also, (VOSSELMAN, 1999) and (ROTTENSTEINER & BRIESE, 2003) show the validity of the plane intersection method for the modeling schemes. Later on, (SCHWALBE ET AL., 2005) adopt specific orthogonal point projection strategy for the reconstruction workflow. The potential of intersection lines and more comprehensive step-edges to the reconstruction steps is again shown by the (ROTTENSTEINER ET AL, 2005). Currently, plane intersection information and as well as topological information are being used for the building reconstruction.

Topological information provides the mutual arrangement and/or relationship between neighboring roof planes. In (2000) AMERI & FRITSCH use Voroni diagrams to obtain the mutual connections between the roof planes. Later, (VERMA ET AL., 2006) adopt the properties of primitive roof shapes by means of the topology. In this approach, it is assumed that any complex building can be decomposed into number of primitive shapes thus the counter recognition of neighboring primitive is the way to model a building for them. Hence, first they recognize the topological relationships among neighboring roofs of a building and represent in a graph. Consequently, sub graph matching is adopted to detect best possible primitive shape to be represented for a set of roof planes. Although ambiguity of the graph matching has been avoided by them, their approach was limited to a few primitive shapes. Later, formal grammar is added to the primitive shapes that have been identified by sub graph matching by (MILDE ET AL., 2008). In addition to the grammar rules, some additional corner connectors have also been used to get a valid roof model. Sub graph matching, introduced by (VERMA ET AL., 2006), is extended by (OUDE ELBERINK, 2010), and used not only various roof primitive types but also the nature of discontinuity changes among roof planes, i.e. status of ridge-line or step-edge lines, for the matching process. Complete matching result, with few incomplete matches, is obtained from some buildings where missing planes are existed. Thus, incomplete matches is attempted to solve by suggesting a best matched option due to the fact that has been arose as a result of the missing data.

Due to the ambiguities of sub graph matching with relevant data features and limitations of defining possible primitive shapes for the matching, we propose a new approach using closed cycle graphs. Consequently, geometrically valid complete roof structures are obtained by avoiding the graph matching process.

2   Roof Plane extraction

ALS points cloud is initially segmented into different planar faces by adopting the method, implemented by (VOSSELMAN ET AL., 2004). Optimum parameters are chosen during the segmentation step as it is crucial, as shown by (DORNINGER & PFEIFER, 2008), in the building reconstruction schemes. Our intention is to follow a rule based extraction strategy for the detection of roof planes as we do not have any clue about the potential building areas. Accordingly, terrain point classification is a prerequisite, which we need to satisfy prior to the roof extraction, for our approach. Since, we already have planar segments; a developed version

of a segment based classification process, presented by (PERERA, 2007) is adopted for the terrain point extraction. Mutual relationships among segments are recognized and presented as an adjacency map; for instance, for neighboring segments A, B and C (see figure 1), their adjacency relationship is taken as (B, C), (A, C) and (A, B) respectively.
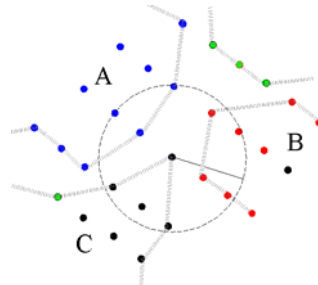

Fig. 1: Mutual connection of segments at an AOI

As the mutual relationship is relied on the spatial distribution of segments, a Delaunay triangulated point neighborhoods are taken at a desired Area of Interest (AOI) to obtain segment adjacencies. This AOI radius is set in a way that accommodate at least one point from the neighboring segments whose minimum distance separation, stay within the distance which we prefer to consider as an adjacent. Discontinuities among the segments are identified and accordingly segments are classified as either terrain or off-terrain. Although, we achieve a good classification results, the terrain point classification is not fully discussed here as it is out of scope of the paper.

Assuming, any complex roof can be recognized by detecting their primitive shapes such as gable, hip and so on, different rules are imposed to detect as much of roof segments from a similar adjacency map. Except isolated flat and shed roofs, most of the other common roofs or part of the roofs might associate with break lines and also individual roof plane might have a certain azimuth difference with respect to the azimuth of the adjacent roof plane. Hence, taking pair of adjacent segments at a time, relative azimuth differences are tested. When the azimuth difference is equal near to the 180 or 0 degree, then segments which follow our horizontality constraint on break line is used to refine potential roof planes.

Nature of the constraint	Threshold	Target roof types
Azimuth difference between adjacent segment pair & Horizontality of break line	$180°±3°$ or $0±3°$ $< 3°$	Gable, mansard
Azimuth difference between adjacent segment pair & Non-horizontality of break line	$90±0°$ $> 3°$	Hip, L-shaped
Slope constraint for oblique roofs	$> 5°$ and $< 75°$	All oblique roofs (including shed)
Slope constraint for the flat roofs	$< 5°$	flat
Height threshold	1.5 meter	For all roof types

Tab. 1: Summary of the parameter for rules on the roof extraction

Moreover, 90 degree azimuth constraint together with oblique ridge-lines constraint is also used to extract some other roof planes. Further to that, oblique roofs, which have not followed our defined azimuth constraints at their given adjacencies and remained adjacent to the previously detected faces, are extracted using the slope constraints; this is in addition to the extraction of individual oblique roofs by the slope constraints. A height threshold well above the terrain is always imposed to reduce the low vegetation being depicted as roof planes. Summary of the parameters that have been adopted for roof plane extraction is given in table 1 and some results, relevant to the above step, are shown in figure 2.

Fig. 2: Raw point clouds (left), planar segments (middle), Extracted roofs (right): cyan & white - building, green – vegetation, red – terrain, black – non segmented point patches

3 Construction of Roof Topology Graph (RTG)

Once the roof plane extraction is completed, adjacency map is updated by removing unwanted segments as they are no longer applicable for the roof reconstruction. Our intention is to generate valid roof structures for every building. Thus, connected components, appear in the updated adjacency map, are taken and assigned a unique building number. Now, a single building represents one or more roof segments in reality, thus, not only outer bounds but also inner bounds are required for the generation of a complete 3D roof structure. In most cases, step-edges and ridge-lines are provided the necessary inner boundary limits of individual roof planes. In contrast, these two discontinuity scenarios (i.e. step-edges and ridge-lines), let's say feature lines, further tells us how each roof resides with respect to the other roof, i.e., topological relationship, in the real building. Hence, topological relationships are important to derive, especially in data driven process, for obtaining the valid 3D roof structures. (VERMA ET AL., 2006; OUDE ELBERINK, 2009) suggest a way of presenting such a topological relationship in a connected graph, called a roof topology graph. Therefore, we construct the feature lines of each building and at the same time create the relevant RTGs.

3.1 Feature line construction

The ridge-line information, relevant to a certain pair of segments, is directly given by our roof extraction algorithm, if the segments have been identified as a valid roof pair. This is an added advantage of our roof extraction process. Although, ridge-lines have already been generated, the ridge-line recognizing strategy is briefly explained now as it helps to differentiate our step-edge detection. Generally, valid ridge-lines, appear in buildings, are given by the intersection of two planes, but spatial distribution of points might not be broken, being a ridge-line in between.

Therefore, boundary points, stay within a narrow buffer zone which is sharing both edges, are chosen to validate whether a ridge-line should be accommodated in-between two roof segments or not. In this case, half of the zone width is equal to the distance which is slightly less than twice the point spacing.

On the other hand, if every boundary point or higher percentage of points spatially separate in Z-direction with their counter border points, then step-edges might be existed. So that, best fitted two line segments (up and down) are necessary to represent each step edge. After generating a step-edge, upper edge is recognized and is rectified based on the dominant plane direction and then transferred its planimetric position to the down edge, assuming the relevant wall is vertical and passing through the upper edge.

3.2 Roof topology graph (RTG)

The definition of a graph G, is given as a pair $G = (V, E)$ of sets, such that $E \subseteq [V]^2$, as explained by (DIESTEL, 2010); where V is 'vertices' (or series of nodes) and E is 'edges' (or series of lines). By the definition, an edge can be represented using two pair of vertices. Considering the graph theory on practical point of view, two roof planes can be taken to represent two vertices or an edge in a RTG. As we have additional information to be represented, the edge can be used to represent topological relationships. In our approach, we use two basic relationship categories i.e. "Ridge-line" and "step-edge". Therefore, a complete RTG of a building can be constructed once all the ridge-lines and step-edges, relevant to the building, are generated.

As we know the correct topological relationships among roof planes, now we can demarcate the roof boundaries.

4   Closed Cycle Analysis

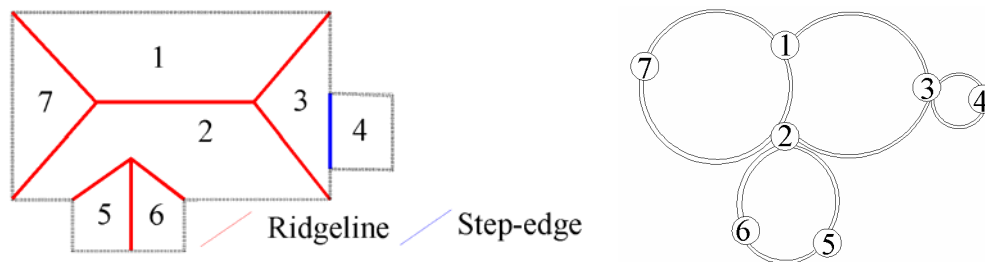Assuming the RTG as a directed graph, the graph G, shown in figure 3, can be described as follows,

Fig. 3: Complex roof structure (left) and derived RTG, G (right)

By the definition, $G = (V, E)$; therefore V={1,3,4,3,2,6,5,2,7} and E={1-3,3-4,4-3,3-2,2-6,6-5,5-2,2-7}. When we traverse over the graph G, different vertices can be chosen to walk in between any two desired end-vertices. Therefore, if the end-vertices are equal to vertex 2 and 1; Then, possible sets of vertices that we could walk are; P1{1,2}, P2{1,2,7}, P3{1,2,3,4,3} and so on., where P1, P2 and P3 are "paths". Hence, we have more than one path to walk in between given end-vertices. When end-vertices are coincided, for e.g. vertex 1, then the path becomes a (closed) cycle. Hence, cycles relevant to the above paths can be rewritten as C1={1,2,1}, C2={1,2,7,1}

and C3={1,2,3,4,3,1}. The length, i.e. number of edges, of each cycle is different and 2, 3 and 5 are the figures for above cases. C1 is appeared as a line, and related to a single pair of roof plane in the RTG. Hence, it can be restricted to analyze such a simple cycle. In addition to that, considering as a shortest path problem, cycles having higher degree of lengths can also be ignored and a unique 'shortest' closed cycle can be obtained for given two end-vertices. Therefore, assuming the RTG has equidistance edges, the well-known Dijkstra's algorithm is applied to distinguish every possible 'shortest' closed cycle, emerged in a complete RTG graph. Hence, identified closed cycles can be used to adjust inner and outer roof bounds of each building.

4.1 Fixing of Ridgeline Intersection

Careful examination of figure 3 shows that the feature lines, relevant to a shortest closed cycle are converged to a single point. Therefore, incidences where the adjacent ridge-lines are supposed to intersect at a single position can be robustly determined by considering every shortest cycle. In this case, as we focus only the ridge-lines, the cycles whose entire edge labels are represented only by the 'ridge-line' category should be chosen. The fixing of such a point can be taken as a least square minimization problem and can be estimated a single position which is closest to all the ridge-lines. We have taken a robust outcome by assigning the weights for each ridge-line as some ridge-lines are more stable than other. Positive weights, lasting from 0 to 1 are assigned, which is directly proportional to the sine value of angle between normal vectors of roof segments. Therefore, without knowing primitive roof types, ridge-lines can be geometrically fixed as shown in figure 4.
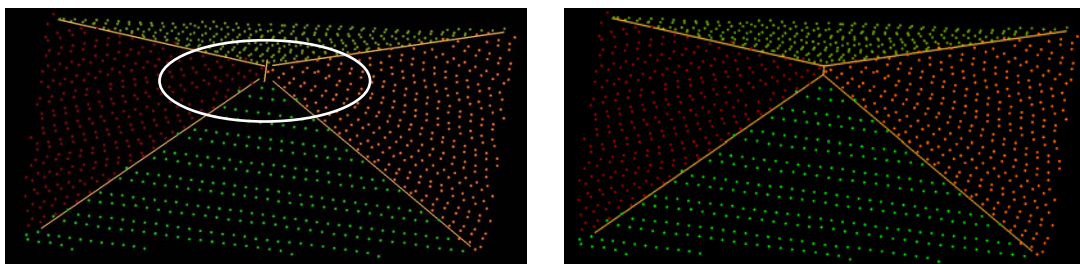

Fig. 4: Ridge-line intersection is fixed: before (left), after fixing (right)

4.2 Fixing, relevant to step-edges

In addition to the ridge-line intersection, many possibilities can be found where step-edge lines themselves and step-edge with ridge-lines suppose to be converged at more than one positions (see, figure 5), holding a same planimetric coordinates with height jumps. Therefore, by analyzing the feature lines together with shortest closed cycles, in a 3D view, a single common position is supposed to construct. Two line segments, referring to two planar faces, are represented by a step-edge. Therefore, presence of the step-edges split the 'cycle' into several 'arcs'. Each arc represents a specific height level of the roof top. As two height levels exist in the figure 5, two arcs or two directed "path graphs" can be used to represent that shortest closed cycle. The splitting of cycles lead to convey in which step edge i.e. either up or down edge, is referred by the particular path graph. Consequently, all the feature lines, relevant to a certain path

graph can be identified, and computed a single intersection point (3D) to represent the corresponding roof corner. However, due to the other path graphs, exist in the same cycle, slightly different planimetric coordinates might be received. Thus, a common planimetric position is taken by averaging each individual position. Transfering of that planemetric coordinate to the other points leads for the geomarically valid roof corners.
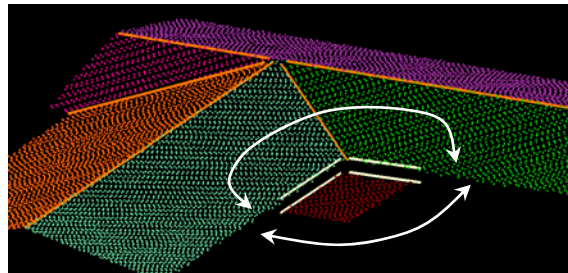

Fig. 5: Step-edges and ridgelines, at a closed cycle, suppose to meet - side view

During the adjustment process, step-edges are allowed to shift by themselves while preserving their directions based on the influence of ridgelines since the ridge-lines are fixed in our approach. Therefore, as in the figure 6, step-edges can be fixed.
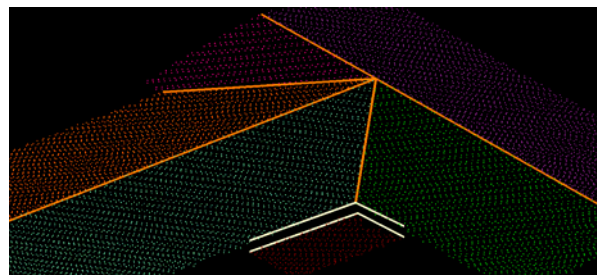

Fig. 6: Convergence of ridgelines and step-edge lines are fixed

4.3   Fixing of Outer Bounds

At this point, entire inner bounds, i.e. inner skeleton, is completely reconstructed and remained with outer bounds. Hence, entire boundary points, relevant to each building or connected components, are extracted by creating the contour of the connected segments. Then, contour is decomposed in to corresponding laser segments and straight lines are fitted to represent every possible deviation, appear within the gutter or eave edges. Distance to fitted line constraint is used to add new points to the line. Once lines are fitted, each line is generalized into orthogonal or parallel direction to the dominant direction of respective roof planes. Still our outer bounds are not coincided with inner skeleton. Therefore, outer ends of skeleton should be adjusted in order to make closed polygon boundaries. In our approach, we suppose to fix the outer ends of inner skeleton using outer most closed cycle of the RTG. For the graph G in figure 3, the outer most cycle can be obtained by taking union of all the sub cycles and the path of the outer cycle can be written with vertices in the order of { 1,3,4,3,2,6,5,2,7,1}. In this case, end-vertex is equal to the vertex 1. Normally, at a roof corner, two outer boundary line segments and an inner bound line (i.e. a feature line) are converged to a single position, and will be the corner position in 3D. Now,

forward walking of the outer cycle and derived list of lines can be used to fix such a roof corner or an end point of an inner skeleton. Hence, corner points can be robustly fixed using respective feature line and two outline segments, resided both sides to the ridge-line or step-edge line. When two intersection points are existed with respective feature line, then most outer point is chosen in order to compensate the size changes of the building foot print. Now, remaining intermediate outlines should be intersected sequentially in order to obtain intermediate turning points that reside in eaves or gutter edges. Finally, a valid 3D roof outline can be obtained.

5   Results and Discussion

Roof structures, shown in figure 7, depict that our experimented method can be used to generate geometrically correct, valid 3D roof boundaries in ALS data. Also, underestimation of the size of the buildings, occur due to the least square line fitting can be reduced in our approach as we enforce to select outer most intersection points during the outline fixing step. Results, in figure 7 further confirm that we can create accurate roof corners. However, some aspect would be needed to improve further, for example when more complicated step-edges are appeared in the roof tops, especially in the flat roofs. According to the roof extraction results, shown in figure 1, it says that some vegetation patches have been misguided our extraction result. Hence, some additional attributes should be adopted to discriminate vegetation patches such as flower beds from the building roofs.
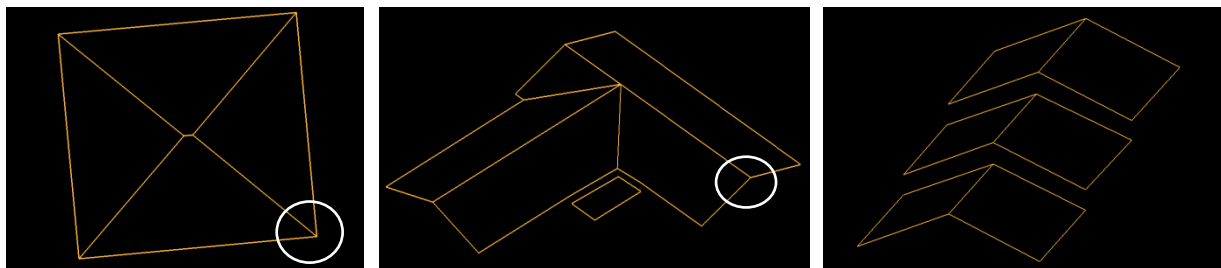

Fig. 7: Sample roof structures: Simple hip roof (left), L-shaped roof with a connected roof by a height jump (middle), Multi-level gable roof (right)

6   Conclusion

This paper presents a new approach to generate 3D roof structures using data driven concepts. The main contribution that we have done is to introduce the usage of cycle graph analysis for obtaining topologically correct roof boundaries. This will be a sound alternative for the limitations of existing sub graph matching process as well. The method can be further improved by integrating 2D building plans or image data. As the method is still being developed, a comprehensive analysis with our developed version of the approach will be discussed in future. In addition to that, the final result of our approach will be assessed by the organizers of the ISPRS Test Project on Urban Classification and 3D Building Reconstruction 2012.

Acknowledgement

The Vaihingen data set was provided by the German Society for Photogrammetry, Remote Sensing and Geoinformation (DGPF) [Cramer, 2010]: http://www.ifp.uni-stuttgart.de/dgpf/DKEP-Allg.html (in German). The authors wish to thank the Organizers of the ISPRS Commission III/4 for distributing the ALS point clouds data and arranging the Test project on Urban Classification and 3D Building Reconstruction.

References

AMERI, B., FRITSCH, D., 2000. Automatic 3D building reconstruction using plane-roof structures, ASPRS, Washington DC.

BRENNER, C., HAALA, N., 1998. Fast reality production of Virtual Reality City Models. IAP, Vol. 32, Part 4.

DIESTEL, R., 2010. Graph Theory. Springer-Verlag, Heidelberg, p. 451.

DORNINGER, P., PFEIFER, N., 2008. A Comprehensive Automated 3D Approach for Building Extraction, Reconstruction, and Regularization from Airborne Laser Scanning Point Clouds. Sensors, **8**(11): pp. 7323-7343.

ISPRS COMMISSION III, 2011, "ISPRS Test Project on Urban Classification and 3D Building Reconstruction".http://www.isprs.org/news/announcements/110314_ISPRS_Intercomparis on-Flyer.pdf (08.01.2012).

MAAS, H.G., AND VOSSELMAN. G., 1999, Two algorithms for extracting building models from raw laser altimetry data, ISPRS Journal of Photogrammetry & Remote Sensing, **54**(2-3): pp. 153-163.

MILDE, J., ZHANG, Y., BRENNER, C., PLUEMER, L. AND SESTER, M., 2008. Building Reconstruction using Structural Description based on a Formal Grammar. In: International Archives of Photogrammetry, Remote Sensing and Spatial Information Sciences, XXXVII, part 3B: pp. 227-232.

OUDE ELBERINK, S., 2009 Target graph matching for building reconstruction. In Laserscanning 2009; International Archives of Photogrammetry, Remote Sensing and Spatial Information Sciences: Paris, France; Vol. 38.

OUDE ELBERINK, S., 2010. "Acquisition of 3d topography: automated 3d road and building reconstruction using airborne laser scanner data and topographic maps," Ph.D. dissertation, University of Twente, Enschede, the Netherlands.

PERERA NIRODHA S., 2007. Segmented based filtering of LASER scanner data, Master thesis, ITC, The Netherlands.

ROTTENSTEINER, F., AND BRIESE, C., 2003. Automatic Generation of Building Models from Lidar Data and the Integration of Aerial Images. In: International Archives of Photogrammetry, Remote Sensing and Spatial Information Sciences, XXXIV, part 3/W13: on CD-ROM.

ROTTENSTEINER, F., TRINDER, J., CLODE, S., AND KUBIK, K., 2005. Automated delineation of roof planes from lidar data. In: International Archives of Photogrammetry and Remote Sensing and Spatial Information Sciences, XXXVI, 3/W19, Enschede, the Netherlands.

SCHWALBE, E., MAAS, H.-G., AND SEIDEL, F., 2005, 3D building model generation from airborne laser scanner data using 2D GIS data and orthogonal point cloud projections. In:

International Archives of Photogrammetry and Remote Sensing and Spatial Information Sciences, Vol XXXVI, Part 3/W19, pp. 209-213.

SOHN, G., AND DOWMAN, I., 2007. Data Fusion of High-Resolution Satellite Imagery and LiDAR Data for Automatic Building Extraction. ISPRS Journal of Photogrammetry and Remote Sensing, 62(1): pp. 43-63.

VERMA, V., KUMAR, R. AND HSU, S., 2006. 3D Building Detection and Modeling from Aerial LIDAR Data, IEEE Computer Society Conference on Computer Vision and Pattern Recognition (CVPR'06). IEEE Computer Society, Washington, DC, USA, pp. 2213-2220.

VOSSELMAN, G., 1999. Building Reconstruction Using Planar Faces in Very High Density Height Data. In: International Archives of Photogrammetry, Remote Sensing and Spatial Information Sciences, XXXII, part 3/2W5: pp. 87-92.

VOSSELMAN, G., B. GORTE, G. SITHOLE AND RABBANI, T., 2004. Recognizing Structure in Laser Scanner Point Clouds. In: International Archives of Photogrammetry, Remote Sensing and Spatial Information Sciences, XXXVI, part 8 / W2: pp. 33-38.